JPEDAV (2010) 31:22–27
DOI: 10.1007/s11669-009-9610-2
1547-7037 ©ASM International

Evaluation of Ti_3Si Phase Stability from Heat-Treated, Rapidly Solidified Ti-Si Alloys

Alex Matos da Silva Costa, Gisele Ferreira de Lima, Geovani Rodrigues, Carlos Angelo Nunes, Gilberto Carvalho Coelho, and Paulo Atsushi Suzuki

(Submitted May 6, 2009; in revised form July 5, 2009)

Ti-base alloys containing significant amounts of silicon have been considered for high temperature structural applications. Thus, information concerning phase stability on the Ti-Si system is fundamental and there are not many investigations covering the phase stability of the Ti_3Si phase, specially its dependence on oxygen/nitrogen contamination. In this work the stability of this phase has been evaluated through heat-treatment of rapidly solidified Ti-rich Ti-Si alloys at 700 °C and 1000 °C. The rapidly solidified splats presented nanometric scale microstructures which facilitated the attainment of equilibrium conditions. The destabilization of Ti_3Si due to oxygen/nitrogen contamination has been noted.

Keywords silicides, Ti alloys, Ti-Si system, Ti_3Si

1. Introduction

Due to their high mechanical strength and low density (~55% of steels), Ti-based alloys have been considered for structural applications at temperatures near 700 °C. Several of these alloys have compositions with significant amounts of Si[1-5] and thus, accurate knowledge of the phase relations in the Ti-Si system, especially in the Ti-rich region is of fundamental importance. The Ti-Si phase diagram shown in Fig. 1[6] indicates the following stable solid phases in the Ti-rich region: (1) terminal αTi-hcp and βTi-bcc solid solutions; (2) Ti_3Si; (3) Ti_5Si_3; and (4) Ti_5Si_4. Among the investigations of this system, there are few focusing on the stability of the Ti_3Si phase. Wakelkamp et al.[7] carried out experiments with Ti-Si alloys and proposed that oxygen contamination played an important role on destabilizing this phase. Suryanarayana et al.[8] carried out heat treatment at 700 °C for 24 h of an initially amorphous $Ti_{80}Si_{20}$ (at.%) alloy and reported to have found an αTi + Ti_5Si_3 microstructure after annealing, which is not in agreement with Fig. 1. In a recent investigation, Ramos et al.[9] claimed to have observed the Ti_3Si phase after heat treating an αTi + Ti_5Si_3 initial microstructure at 1100 °C for 90 h. However, the Ti_3Si phase was not observed after annealing this same alloy composition at 1000 °C for 90 h. In order to contribute to the matter of Ti_3Si phase stability, this work presents results of microstructural characterization of rapidly solidified and annealed (700 °C, 1000 °C) Ti-Si alloys which confirms the stability of the Ti_3Si phase and shows that oxygen/nitrogen doping strongly affects the phase relations in the Ti-rich region of the Ti-Si system. Rapid solidification was employed in order to produce very fine initial microstructures to facilitate the attainment of equilibrium conditions.

Alex Matos da Silva Costa, Carlos Angelo Nunes, and **Paulo Atsushi Suzuki**, Departamento de Engenharia de Materiais (DEMAR), Escola de Engenharia de Lorena (EEL), Universidade de São Paulo (USP), Caixa Postal 116, 12600-970, Lorena, São Paulo, Brazil; **Gisele Ferreira de Lima**, Departamento de Engenharia de Materiais, Centro de Ciências Exatas e de Tecnologia, Universidade Federal de São Carlos, Rod. Washington Luiz, Km 235, Caixa-Postal: 676, 13565-905, Sao Carlos, São Paulo, Brazil; **Geovani Rodrigues**, UniFoa, Centro Universitário de Volta Redonda, Núcleo de Pesquisa, Campus Três Poços, Avenida Paulo Erlei Alves Abrantes, 1325, Bairro três Poços, 27240-560, Volta Redonda, Rio de Janeiro, Brazil; **Gilberto Carvalho Coelho**, Departamento de Engenharia de Materiais (DEMAR), Escola de Engenharia de Lorena (EEL), Universidade de São Paulo (USP), Caixa Postal 116, 12600-970, Lorena, São Paulo, Brazil and UniFoa, Centro Universitário de Volta Redonda, Núcleo de Pesquisa, Campus Três Poços, Avenida Paulo Erlei Alves Abrantes, 1325, Bairro três Poços, 27240-560, Volta Redonda, Rio de Janeiro, Brazil. Contact e-mail: cnunes@demar.eel.usp.br.

2. Experimental Procedure

Ingots (~5 g) of $Ti_{87}Si_{13}$, $Ti_{83}Si_{17}$, and $Ti_{80}Si_{20}$ alloys were initially produced from commercially pure Ti foil (min. 99.3) and Si pieces (min. 99.999) in a water-cooled copper crucible via arc-melting under a gettered argon atmosphere. Five melting steps were carried out to ensure chemical homogeneity. Samples of ~0.1 g were then removed from the ingots and arc-melted to produce near spherical shape samples suitable for levitation in the rapid solidification apparatus. Several rapidly solidified splats of each alloy composition were produced under argon in a splat-cooling apparatus (Edmund Bühler GmbH). The steps of levitation, melting, and splat-formation were easily accomplished with these alloy compositions. Considering the reported sensitivity of phase equilibria in this system with respect to oxygen, the splats were separately encapsulated under argon in quartz tubes together with a significant amount of Ti fillets to act as an $O_2/H_2O/N_2$ getter. The heat treatment conditions were 700 and 1000 °C

for various time ranging from 6 to 90 h. Upon conclusion of the experiments, the capsules were removed from the furnace and air cooled.

The resultant materials had their microstructures characterized by x-ray diffraction (XRD), conventional scanning electron microscopy (SEM), and a selected sample via field-emission gun-scanning electron microscopy (FEG-SEM), using in all cases back scattered electrons (BSE) to form the images. The XRD experiments were performed with a Shimadzu model XRD6000 diffractometer at room temperature, using Ni-filtered CuKα (λ = 1.5418 Å) radiation. The diffractograms of the splats and heat-treated splats were from bulk (x-ray beam incident on one of the surfaces). The phases in the materials were identified by comparing the experimental diffractograms with simulated diffractograms of the phases using the PowderCell program[10] and crystallographic data from Villars and Calvert.[11]

3. Results and Discussion

The accumulated mass losses due to the ingot and spheres production steps were lower than 1%, allowing us to conclude that the nominal compositions were kept. The XRD diffractograms of all sphere materials indicated only the presence of αTi and Ti_5Si_3 phases, an expected result from Fig. 1.

The thicknesses of the produced splats varied in the 58 to 82 μm range. The diffractograms of all splats of a given composition were very similar, indicating a good reproducibility of the rapid solidification process. Figure 2(a-c) shows the XRD diffractograms of the splats (after rapid solidification) from the different alloys (x-ray beam incident on the surface). The diffractogram of the $Ti_{87}Si_{13}$ alloy (Fig. 2a) shows βTi, αTi, and Ti_5Si_3 phases, with a preferential orientation of the βTi phase in the <110> direction. It indicates the formation of crystalline phases for this composition and the retention at room temperature of the high temperature bcc form (β) of Ti due to the high cooling rates achieved in the process. However, when we observed the powder x-ray diffractogram of this splat, only reflections from αTi and Ti_5Si_3 were noted, suggesting that the βTi phase was formed only near the surface of the splat, where higher cooling rates were achieved. The lattice parameter of the βTi phase was approximately 2.15% smaller than that of pure βTi, considering the formation of a substitutional solid solution it could be related to the smaller atomic radius of Si compared to Ti (Si: 117 pm; Ti: 147 pm).

The formation of nanocrystalline/amorphous materials should have occurred in the case of the $Ti_{83}Si_{17}$ and $Ti_{80}Si_{20}$ alloys according to their diffractograms shown in Fig. 2(b) and (c), a result in line with those from Suryanarayana et al.[8] These authors claim the production of amorphous Ti-Si alloys after melt-spinning for compositions in the 15 to 20% Si range.

The conventional SEM/BSE micrographs from a splat of $Ti_{87}Si_{13}$ composition showed two distinct regions in the cross section, one corresponding to those initially solidified from the contact of the liquid with the copper anvils and appeared to be single-phase at SEM resolution. The second one corresponded to the central part of the splat and showed a very fine equiaxed microstructure (<0.1 μm).

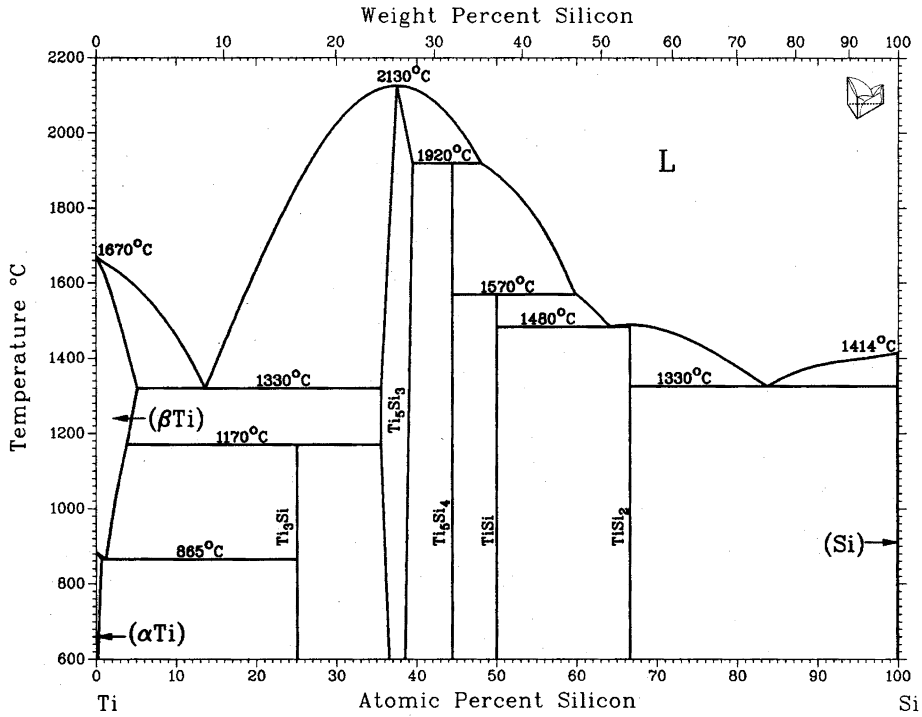

Fig. 1 Phase diagram of the Ti-Si system[6]

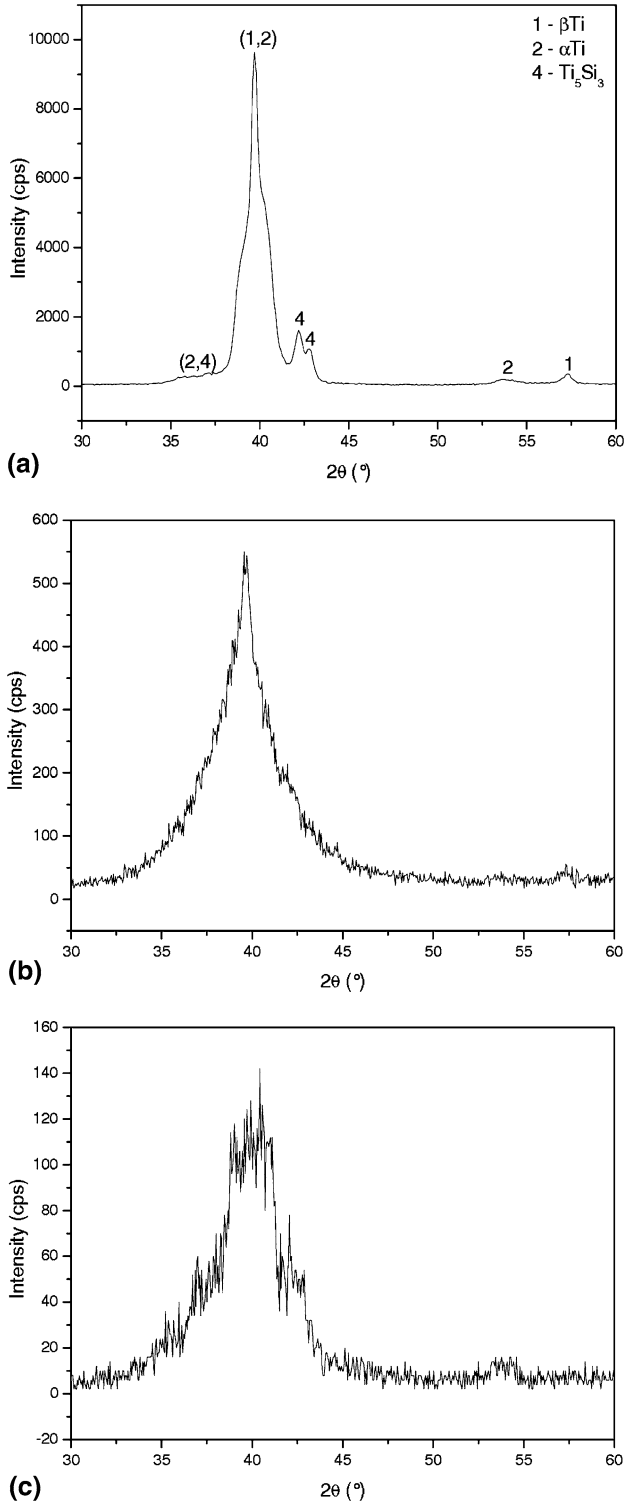

Fig. 2 X-ray diffractograms of the splats (x-ray beam incident on the surface): (a) $Ti_{87}Si_{13}$; (b) $Ti_{83}Si_{17}$; and (c) $Ti_{80}Si_{20}$

However, SEM-FEG/BSE analysis did not suggest important microstructural differences between these two regions. Figure 3(a, b) shows SEM-FEG/BSE micrographs from the central part of a splat of $Ti_{87}Si_{13}$ composition indicating the

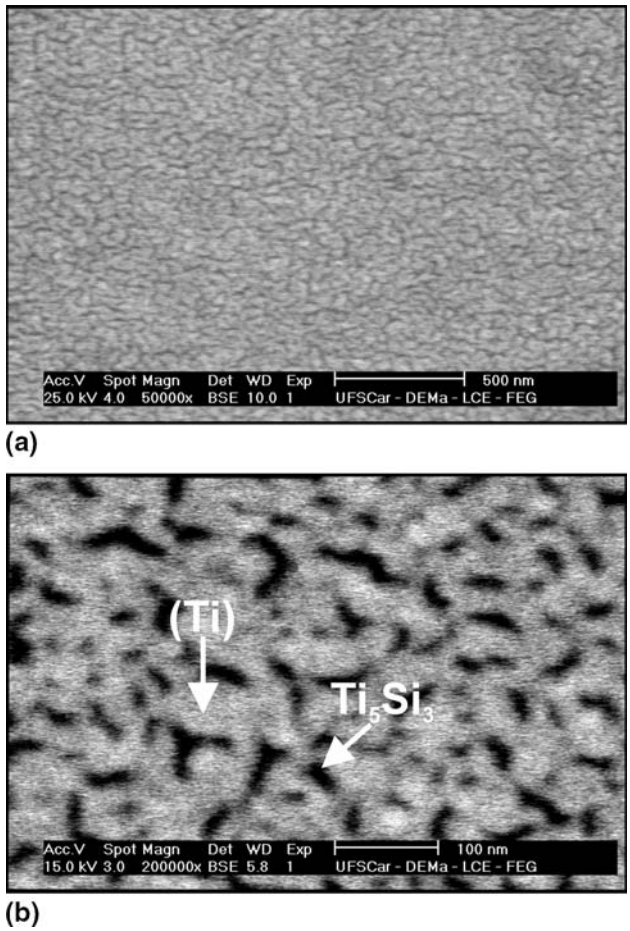

Fig. 3 SEM-FE/BSE micrographs of the cross section of a splat of $Ti_{87}Si_{13}$ composition: (a) lower magnification; (b) higher magnification

existence of two phases of nanometric size, which should correspond to αTi and Ti_5Si_3, based on the XRD results (Fig. 2a).

Figure 4 presents the x-ray diffractograms (x-ray beam incident on the surface) from the splats of the $Ti_{87}Si_{13}$ composition after heat-treatment at 700 °C for 90 h (Fig. 4a) and 1000 °C for 6 h (Fig. 4b). Both diffractograms indicate the presence of αTi and Ti_3Si, suggesting the occurrence of the βTi ↔ αTi transformation and Ti_3Si formation (Ti_5Si_3 + α/βTi ↔ Ti_3Si) during heat-treating. These results were confirmed via EDS analysis of these splats whose cross section SEM/BSE micrographs are shown in Fig. 5, noting disperse Ti_3Si particles embedded in a αTi matrix. Note also the appreciably larger size of the Ti_3Si particles in the material heat-treated at 1000 °C (~3 μm) compared to that heat-treated at 700 °C (<1 μm). As noted previously, Ramos et al.[9] have not observed Ti_3Si formation during heat-treatment (1000 °C/90 h) of an arc melted alloy of same composition, which shows the beneficial effect of the fine initial microstructure provided by the rapid solidification process used in this work to produce equilibrium microstructures.

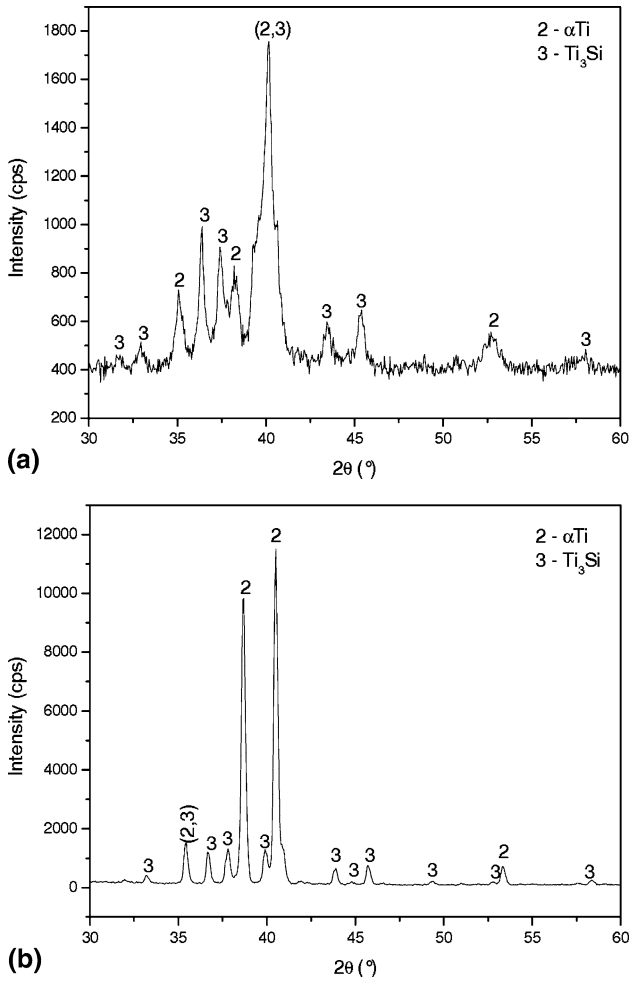

Fig. 4 X-ray diffractograms (x-ray beam incident on the surface) of heat-treated splats of $Ti_{87}Si_{13}$ composition. Use of Ti fillets as getter in the quartz capsules: (a) 700 °C for 90 h; (b) 1000 °C for 6 h

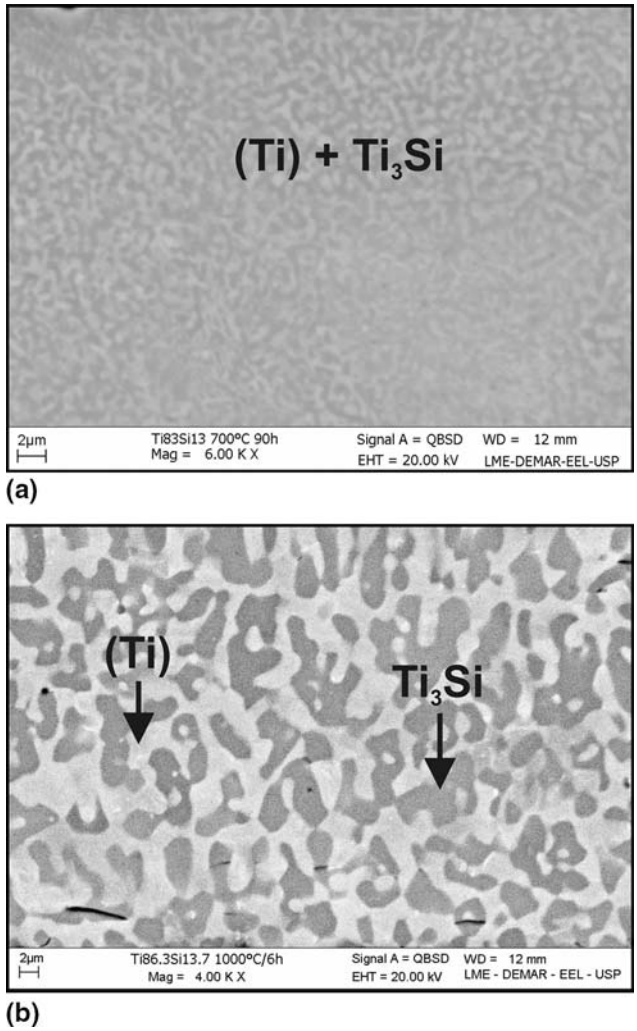

Fig. 5 SEM/BSE micrographs of the cross section of heat-treated splats of $Ti_{87}Si_{13}$ composition. Use of Ti fillets as getter in the quartz capsules: (a) 700 °C for 90 h; (b) 1000 °C for 6 h

The results from the heat-treated splats of $Ti_{80}Si_{20}$ composition were similar to the previous alloy, i.e., it also showed the presence of αTi and Ti_3Si (Fig. 6). However, in this case, the αTi particles are embedded in a Ti_3Si matrix as shown in the cross section SEM/BSE micrographs of this alloy given in Fig. 7. Several particles of the αTi phase are much larger (∼3 μm) in the material heat-treated at 1000 °C compared to that heat-treated at 700 °C (<1 μm), suggesting the occurrence of an important coarsening process at the higher temperature.

In order to evaluate the effect of minor amounts of oxygen/nitrogen on the phase stability of these alloys, one splat of the $Ti_{87}Si_{13}$ composition was encapsulated in a quartz tube under argon, without the fillets of Ti getter. Figure 8 shows a cross section of the splat heat-treated at 1000 °C for 10 h, where only αTi and Ti_5Si_3 are present, clearly showing the stabilization of the Ti_5Si_3 phase due to minor oxygen/nitrogen doping. During heat-treating, due to the very fine size of the Ti and Ti_5Si_3 particles, in the central part of the splat Ti_3Si should have formed, since some time was necessary for oxygen/nitrogen to diffuse from the surface to the central part. Subsequently, the Ti_3Si in these regions are destabilized and transformed to Ti_5Si_3 upon the arrival of the oxygen/nitrogen atoms.

4. Summary

The stability of the Ti_3Si phase has been evaluated in this work by means of heat-treated rapidly solidified Ti-Si alloys. The production of very fine microstructures facilitated the attainment of equilibrium conditions where the Ti_3Si could be observed in samples carefully heat-treated at 700 and 1000 °C to avoid oxygen/nitrogen contamination. On the other hand, the Ti_3Si did not form during heat-treatments where minor amounts of oxygen/nitrogen were present, showing the high sensitivity of the phase relations

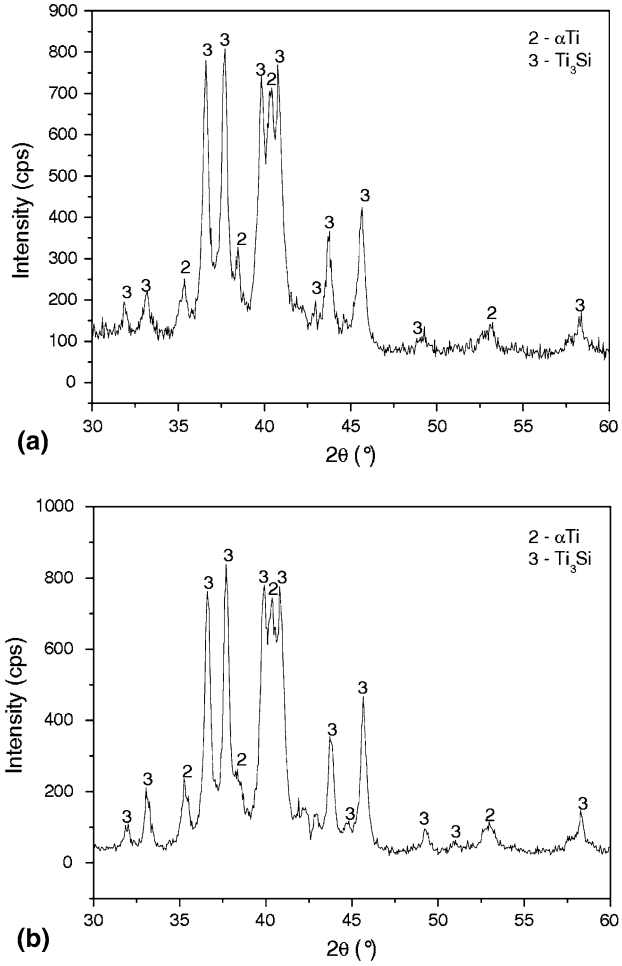

Fig. 6 X-ray diffractograms (x-ray beam incident on the surface) of heat-treated splats of $Ti_{80}Si_{20}$ composition. Use of Ti fillets as getter in the quartz capsules: (a) 700 °C for 52 h; (b) 1000 °C for 20 h

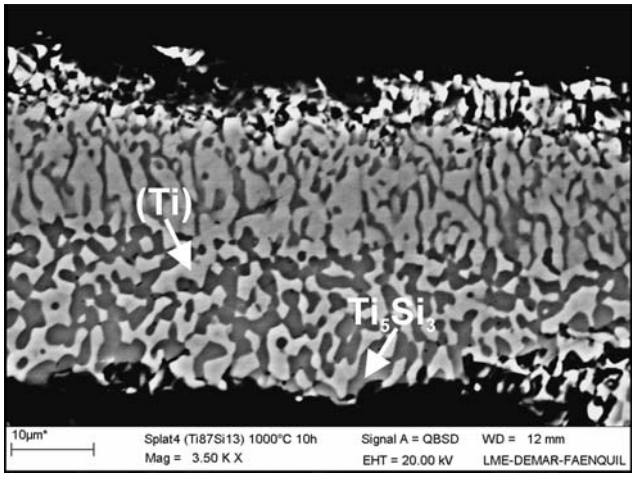

Fig. 8 SEM/BSE micrograph of the cross section of a splat of $Ti_{87}Si_{13}$ composition heat-treated at 1000 °C for 10 h. No use of Ti fillets as getter in the quartz capsule

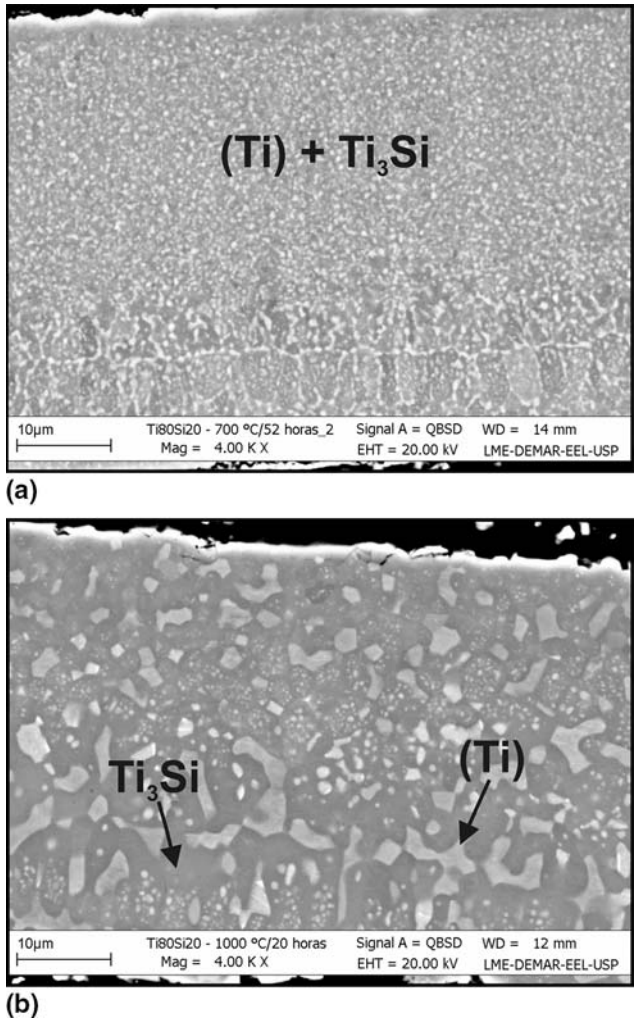

Fig. 7 SEM/BSE micrographs of the cross section of heat-treated splats of $Ti_{80}Si_{20}$ composition. Use of Ti fillets as getter in the quartz capsules: (a) 700 °C for 90 h; (b) 1000 °C for 6 h

in the Ti-rich corner of the Ti-Si system with respect to oxygen/nitrogen contamination.

References

1. Y. Zhan, Z. Sun, J. Jiang, J. Ma, and Q. Guo, Isothermal Oxidation Behavior of Ti-Si Eutectic Alloys with Ai, and Nb Addition, *Corrosion*, 2008, **64**(11), p 845-853
2. Y. Zhan, Y. Wang, J. Ma, L. He, Z. Yu, and H. Xie, Microstructural Characteristics and Elevated Temperature Wear of Ti-11Si-16Al Alloy, *Int. J. Mater. Res.*, 2008, **99**(1), p 75-83
3. A.V. Masur, M.M. Gasik, and V.I. Mazur, Microstructure Formation in Ti-Si Composite Subjected to High Temperature Gradients, *Z. Metallkd.*, 2005, **96**(4), p 377-379
4. D. Vojtech, B. Bártová, and T. Kubatik, High Temperature Oxidation of Ti-Si Alloys, *Mater. Sci. Eng.*, 2003, **A361**, p 50-57
5. H. Wu, Y.F. Han, Y.B. Zhou, and X.C. Chen, Microstructure and Fracture Mechanisms of Ti-Si Eutectic Alloys, *Metallofiz. Nov. Tekh.*, 2002, **24**(12), p 1697-1704

6. B. Massalski, P.R. Subramanian, and H. Okamoto, *Binary Alloy Phase Diagrams*, ASM, Metals Park, 1990, p 3367-3371
7. W.J.J. Wakelkamp, F.J.J. van loo, and R. Metselaar, Phase Relations in the Ti-Si-C System. *J. Eur. Ceram. Soc.*, 1991, **8**(3), p 135-139
8. C. Suryanarayana, A. Inoue, and T. Masumoto, Transformation Studies and Mechanical Properties of Melt-Quenched Amorphous Titanium-Silicon, *J. Mater. Sci.*, 1980, **15**, p 1993-2000
9. A.S. Ramos, C.A. Nunes, and G.C. Coelho, On the Peritectoid Ti_3Si Formation in Ti-Si Alloys, *Mater. Charact.*, 2006, **56**, p 107-111
10. W. Kraus and G. Nolze, Powder Cell—A Program for the Representation and Manipulation of Crystal Structures and Calculation of the Resulting X-ray Powder Pattern, *J. Appl. Cryst.*, 1996, **29**(3), p 301-303
11. P. Villars and L.D. Calvert, *Pearson's Handbook of Crystallographic Data for Intermetallic Phases*, 2nd ed., ASM International, Materials Park, 1991, four volumes